Bioresource Technology 390 (2023) 129880

Contents lists available at ScienceDirect

Bioresource Technology

journal homepage: www.elsevier.com/locate/biortech

Autotrophic production of polyhydroxyalkanoates using acidogenic-derived H_2 and CO_2 from fruit waste

Paolo Costa [a,b], Marina Basaglia [a], Sergio Casella [a], Christian Kennes [b], Lorenzo Favaro [a,*,1], María C. Veiga [b,1]

[a] Department of Agronomy Food Natural resources Animals and Environment (DAFNAE), Waste to Bioproducts-Lab, Università di Padova, Agripolis, Viale dell'Università 16, Legnaro, Padua 35020, Italy

[b] Chemical Engineering Laboratory, Faculty of Sciences and Centre for Advanced Scientific Research (CICA), University of A Coruña, Rúa da Fraga 10, Coruña 15008 A, Spain

HIGHLIGHTS

- First reported evidence of PHA autotrophic accumulation from biogenic H_2 and CO_2.
- Under autotrophic conditions, *C. necator* DSM 545 increased 3HB accumulation of 42%.
- Two reactors: *(i)* acetogenesis of melon waste; *(ii)* H_2 and CO_2 fermentation in PHA.
- To boost H_2 and CO_2, methanogenesis was stopped and OLR increased to 20 gCOD/L/d.
- 13 gCOD/L of VFAs and alcohols were also produced and converted into 3HB and 3HV.

GRAPHICAL ABSTRACT

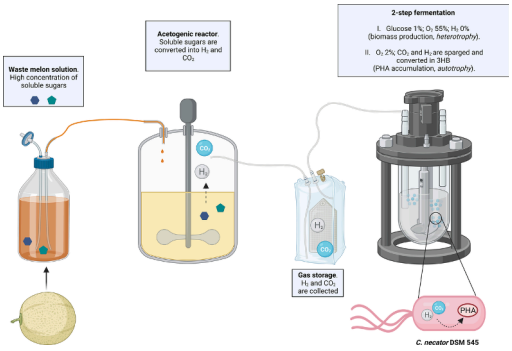

ARTICLE INFO

Keywords:
Two-step fermentation
Cupriavidus necator
Gas fermentation
Dark fermentation
PHAs

ABSTRACT

The environmental concerns regarding fossil plastics call for alternative biopolymers such as polyhydroxyalkanoates (PHAs) whose manufacturing costs are however still too elevated. Autotrophic microbes like *Cupriavidus necator*, able to convert CO_2 and H_2 into PHAs, offer an additional strategy. Typically, the preferred source for CO_2 and H_2 are expensive pure gases or syngas, which has toxic compounds for most PHAs-accumulating strains. In this work, for the first time, H_2 and CO_2 originating from an acidogenic reactor were converted autotrophically into poly(3-hydroxybutyrate) P(3HB). During the first stage, a mixed microbial community continuously catabolized melon waste into H_2 (26.7 %) and CO_2 (49.2 %) that were then used in a second bioreactor by *C. necator* DSM 545 to accumulate 1.7 g/L P(3HB). Additionally, the VFAs (13 gCOD/L) produced during acidogenesis were processed into 2.7 g/L of P(3HB-*co*-3HV). This is the first proof-of-concept of using acidogenic-derived H_2 and CO_2 from fruit waste to produce PHAs.

* Corresponding author.
E-mail address: lorenzo.favaro@unipd.it (L. Favaro).
[1] These authors equally contributed to the work and shared last authorship.

https://doi.org/10.1016/j.biortech.2023.129880
Received 15 September 2023; Received in revised form 14 October 2023; Accepted 14 October 2023
Available online 16 October 2023

1. Introduction

The manufacture of virgin fossil-based plastics is not curbing, yet conversely, their market volume increases exponentially, hence seriously jeopardizing the environment (Geyer et al., 2017). Thereby, besides revolutionizing the existing waste management, it becomes crucial to increase the fraction of bioplastics. Among these polymers, polyhydroxyalkanotes (PHAs) could represent one of the most promising solutions (Bhatia et al., 2021). PHAs are bio-based and biodegradable plastic materials that accumulate intracellularly by several microorganisms in the form of granules and function as a carbon reservoir in case of stressful conditions (Obruca et al., 2021). Interestingly, PHAs can be exploited to obtain commodities for multiple applications, symmetrical to fossil-based plastic ones. However, the high costs of carbon substrates still constrain severely PHAs costs and their commercialization (Yadav et al., 2020); thus a great portion of researchers' efforts is pointed towards the quest for low-cost substrates (Favaro et al., 2019; Ganesh Saratale et al., 2021; Yukesh Kannah et al., 2022).

In this sense, recently, gaseous feedstocks gained great interest, giving birth to 3rd generation bioplastics (Koch et al., 2023). Briefly, three main metabolisms drive C1 gases assimilation: (i) CO_2 enters the Calvin-Benson-Bassham (CBB cycle) in cyanobacteria, which receive energy from light, and in non-photoautotrophic bacteria, like *Cupriavidus necator*, that obtain instead energy from H_2; (ii) the Wood-Ljungdahl pathway (WLP) allows the conversion of both CO_2 and CO in other autotrophic bacteria such as *Acetobacterium woodi*; (iii) CH_4 is metabolized through the serine cycle combined with the ethylmalonyl-CoA pathway (EMCP) in type II methanotrophic bacteria like *Methylocystis* sp. (Yoon and Oh, 2022).

A rich source of C1 gases is syngas (synthetic gas) that originates from processes like blast furnaces or pyrolysis and it is generally composed of 40 % CO, 40 % H_2, 10 % CO_2 and 10 % N_2 respectively (Liu et al., 2014). The high content of greenhouse gases renders syngas extremely polluting, but, at the same time, a potential cost-effective feedstock for PHAs production (Nangle et al., 2020). However, some critical issues limit syngas utilization and in general gas utilization. Firstly, gas mixtures contain H_2 that encompasses an explosive potential, especially if combined with O_2. This constrains the use of aerobic PHAs-accumulating microbes, since either O_2 is kept below the explosion limit (around 4–6.9 %) curbing biomass production, or H_2, that fuels the CBB cycle, is provided only at very low levels (Miyahara et al., 2020). Indeed, when the autotrophic production of PHAs from a low-H_2 gas mix and under aerobic conditions was addressed, the obtained yields were very limited (Miyahara et al., 2020). As an alternative, a two-step process was proposed: first, a large microbial growth was obtained using glucose or glycerol in aerobic conditions, afterwards the same biomass accumulated PHAs from a mix of H_2: O_2: CO_2 = 84: 2.8: 13.2 (vol%) (Garcia-Gonzalez et al., 2015). Nevertheless, O_2 mass transfer still limited PHAs biosynthesis. Continuous stirred tanked reactors (CSTR) such as gas-lift bioreactors could be an alternative to increase the volumetric mass transfer coefficient (k_La) and boost the yields (Riegler et al., 2019). In addition, when it comes to syngas, CO is converted into PHAs at too low rates by native CO-utilizing bacteria, while it represents a heavily toxic compound for the large majority of strains (Yoon and Oh, 2022).

C. necator, an extremely studied Gram-negative β-proteobacterium (Brojanigo et al., 2022b; Mukherjee and Koller, 2023), oxides H_2 through membrane-bound hydrogenases: as a result, H^+ atoms and electrons are transported in the respiratory chain, generating ATP and NAD(P)H that fuel CBB cycle. Within this metabolic pathway, CO_2 is converted by rubisco in 3-phosphoglycerate (3-PG) that in turn is transformed into phosphoenolpyruvate which eventually becomes pyruvate and enters the Krebs cycle. Specifically, four carbonic anhydrase-like (CA-like) enzymes are expressed by *C. necator* entailing large amounts of CO_2 to be fixed by a highly specific rubisco variant. Additionally, whether rubisco generates toxic 2-phosphoglycolate, this is recycled by a glycerate cycle into 3-PG to re-enter the CBB cycle (Panich et al., 2021). Indeed, *C. necator* has been chosen to produce autotrophically several chemicals such as isopropanol and methyl ketones (Liu et al., 2016; Müller et al., 2013). For what concerns the autotrophic production of PHAs, *C. necator* recorded 1.55 g/L/h productivity of poly (3-hydroxybutyrate), P(3HB), using a doughnut-shaped basket-type agitator (Tanaka et al., 1995). Similarly, monitoring the diffusion of O_2 and CO_2, the dosage of the gas mixture was optimized, hence up to 15 g/L of cell dried matter with 77 % of P(3HB) were accumulated using *C. necator* H16 DSM 428 (Lambauer et al., 2023; Lambauer and Kratzer, 2022).

This work proposes an alternative strategy to address autotrophic production of PHAs, avoiding the use of CO-rich syngas or more expensive pure gases which require purification pre-treatments. Specifically, an acidogenic reactor (AR) was selected as the key pre-treatment of food waste to obtain both H_2 and CO_2. As such, the gaseous effluent originating from an AR fed with melon waste, composed of a mix of H_2 and CO_2, was efficiently converted into P(3HB) by *C. necator* DSM 545. The Organic Loading Rate (OLR) was finely tuned to optimize the release of H_2 and CO_2 from the AR, then a two-step PHAs production was set up: after biomass growth, either liquid or gaseous streams from the AR were transformed into PHAs. To the best of the authors' knowledge, this work reports for the first time the successful conversion of H_2 and CO_2 from acidogenesis into PHAs. This novel approach paves the way of exploiting acidogenic-derived CO_2 and H_2 as clean and cheap feedstock for PHAs production.

2. Materials and methods

2.1. Microorganism and substrate preparation

For continuous-operating AR, fed with melon waste, the biomass used was an anaerobic sludge collected from the anaerobic digester of a brewery wastewater treatment plant. *C. necator* DSM 545, supplied by DSMZ (Braunschweig, Germany), was maintained at −80 °C in 25 % glycerol stock solution and plated on nutrient agar Petri dishes when needed (g/L: peptone 15, yeast extract 3, NaCl 6, glucose 1, agar 15).

Twenty kg of melons discarded by the supply chain were kindly donated by FRANCESCON OP SOC.AGR. SOC.CONS. a.r.L. Whole melons were ground, frozen at −20 °C, and freeze-dried for 48 h. Afterwards, the resulting melons were ground using a ring mill and sieved using laser granulometry to obtain different particle sizes. As a result, 90 % of the obtained particle size was below 500 μm and used for acetogenic experiments, while the rest was discarded to avoid pump clogging.

2.2. Continuous production of H_2 and CO_2 in melon-fed reactor

Acidogenic fermentation was carried out in a 2L anaerobic sequencing batch reactor (AnSBR). The bioreactor was fed with a continuously stirred stock solution of melon resuspended in tap water and autoclaved. The bioreactor working volume was 1L and, at the end of every cycle (1 or 2 per day) 50 % of the volume was removed and substituted with a fresh melon solution. The OLR ranged between 5 and 20 gCOD/L d, according to melon solution organic loading OL (10 or 20 g COD/L) and Hydraulic Retention Time (HRT) (48 or 24 h). Before inoculating the reactor, to inhibit archaeal strains responsible for methane production, the inoculum was pre-treated at 100 °C for 4 h (Tagne et al., 2023). In this way, archaeal strains were inhibited, and anaerobic digestion was stopped at the acidogenic phase to boost H_2 and CO_2 synthesis. To further increase H_2 production, pH was maintained at 5.5 by adding NaOH, as it was previously reported that hydrogenase catalytic activity is optimized when pH is around 5.5, and hydrogen production is thus favored (Alibardi et al., 2012; Favaro et al., 2013). Additionally, the melon solution was supplemented with 2-Na-bromoethanesulfonate (BES) 10 mM. Indeed, BES is a structural analogue, and thereby competitor, of the coenzyme M which presents the methyl group

to the methyl-Co-M reductase enzyme when methane is produced (Waghmode et al., 2015). By supplementing BES, CH_4 synthesis is strongly inhibited. After inoculation, the reactor was sparged with pure N_2, and temperature maintained at 37 °C by circulating water through the reactor glass jacket. The reactor was stirred at a constant rate by a mechanical agitator. which was stopped for 1 h before every volume removal to let biomass settle down. The headspace was connected to a flow meter first to measure total gas production and eventually to a plastic balloon to collect the whole gaseous stream. The three tested ORLs (5, 10, and 20 gCOD/L/d) were compared in term of bioconversion rate (Greses et al., 2021) using the following equation:

$$\text{Bioconversion}\,(\%) = \frac{VFAs\ and\ alcohols\ (effluent)}{COD\ (influent)}100$$

2.3. PHAs production by C. necator DSM 545 from acidogenic reactor gaseous or liquid effluents

To obtain the inocula for bioreactor fermentations, *C. necator* DSM 545 was grown at 30 °C in 5 mL Nutrient broth. After 24 h, 2 mL were washed with NaCl 0.9 % and seeded for 24 h in 250 mL flasks containing 100 mL 10-times concentrated DSMZ-81 broth (Rodríguez Gamero et al., 2018) and glucose 3 %. The experiments were carried out in a 2 L BIOSTAT B-PLUS bioreactor (Sartorius-BBI-Systems, PA, USA) using a working volume of 1.5 L. Eventually, the vessel was autoclaved at 120 °C for 20 min, then the sterile medium was added and, at last, the reactor was inoculated with 0.3 starting optical density (OD_{600}).

To test PHAs production, a two-stage fermentation strategy was adopted. During the first phase, biomass grew for 48 h at 30 °C on DSMZ-81 and glucose 3 %. Oxygen saturation was maintained at 55 % by sparging pure O_2; stirring and pH were kept at 450 rpm and 6.8 adding NaOH, respectively. No antifoam was needed. Afterwards, cells were pelleted and resuspended in the same medium, deprived of NH_4Cl to increase the C/N ratio, favoring PHAs accumulation conditions. Glucose was not added, while either gaseous or liquid streams from the AR were supplemented, where CO_2 or volatile fatty acids (VFAs) and alcohols were the carbon sources, respectively. On the other hand, in the control experiment, during the second phase of fermentation, besides the depletion of NH_4Cl, to estimate the real contribution of the gaseous or liquid streams from the AR, no carbon source was provided. The accumulation phase was extended for 48 h and, because of H_2 presence in autotrophic conditions, O_2 saturation level was kept below the lower explosion limit at 2 % (v/v) for all the tested conditions. Specifically, the content of the plastic balloon collecting gas from AR was sparged into PHAs reactor every 24 h. Each supplementation was preceded by gas volume and composition measurements with a fluxmeter and gas chromatography (GC), respectively. As no traces of other gases but H_2, CO_2, and N_2 were detected with the GC, it was not conduced a control experiment with an artificial mix of gases replicating the fractions of H_2 and CO_2 measured for the autotrophic experiment. On the other hand, when the liquid effluent was tested, this was cleaned from any solid fraction by centrifugation and then autoclaved. Experiments were conducted in duplicate.

2.4. Analytical procedures

Cellulose, hemicellulose, lignin, starch, and protein composition were evaluated in freeze-dried melon according to international standard methods (Basaglia et al., 2021). The dry matter and ashes content was evaluated by drying the samples at 105 °C for 24 h and at 550 °C for 2 h, respectively (Brojanigo et al., 2020). Simple sugars, VFAs and alcohols contents of melon solution feeding the AR and relative liquid effluents were analyzed by high-performance liquid chromatography (HPLC) employing a Hewlett Packard chromatograph (HP1100 Series, Agilent Co., USA), an Agilent Hi-Plex Column (300×7.7 mm) and both a diode array detector (DAD) and a refractive index detector (RID) maintained at 50 °C. The sugars conversion (%) calculation was based on the sugars content both in the feeding and in the effluent solutions. Carbon oxygen demand (COD), volatile suspended solids (VSS) of melon, and samples from AR, as well as soluble ammonium, were calculated following Standard Methods (APHA, 2012). Solids retention time (SRT) was calculated from VSS of the mixed reactor and of the liquid effluents after biomass settlement, and specific volumes were purged from the mixed reactor accordingly. Gas composition was measured using a gas chromatograph containing a Poropack-Q column and a thermal conductivity detector (TCD) as well as a gas chromatograph (490 Micro GC, Agilent Technologies, CA, USA) equipped with a thermal conductivity detector (TCD) and two different capillary columns, one using argon as carrier gas and the other using helium, operating at 145 °C, 30 psi and 100 °C, 28 psi, respectively (Tagne et al., 2023). On the other hand, PHAs were extracted from freeze-dried pelleted cells and the PHA content was measured by gas chromatography to detect 3-hydroxybutyrate (3HB) and 3-hydroxyvalerate (3HV) monomers (Abbondanzi et al., 2017; Brojanigo et al., 2022a). Finally, total organic nitrogen of PHAs reactor media was measured, while elemental analysis for total carbon, nitrogen and hydrogen of freeze-dried melon was performed using an Elemental Analyzer FlashEA112 (ThermoFinnigan).

3. Results and discussion

3.1. Substrate choice and characterization

In a previous study, melon waste was found to be a promising P(3HB-*co*-3HV) feedstock (Costa et al., 2022). Melon is largely available in Southern Europe, where Italy and Spain are leaders in terms of production quantity: both countries every year produce around 600 kT according to FAOSTAT (Food and Agriculture Organization Statistics). In this work, one of the goals was also to test whether melon might accordingly represent a promising waste for H_2 and CO_2 production. Table 1 summarizes the characteristics of the 20 kg melon batch used for the following experiments. Data are referred to melon after freeze-drying, a process that caused 89.6 % of weight loss. Differently, soluble sugars HPLC measurements were run on samples from the melon solution used to feed the AR, after autoclaving.

The high values in terms of dried matter, VSS and COD, reflect the lack of water in freeze-dried samples. Free sugar concentration reaches up to almost 30 % of melon dried weight, suggesting that nutrients extraction in water is a technique as simple as efficient, thereby promising for various biotransformation. Additionally, while a 15 % fraction is represented by proteins, a further 20 %, despite the total lack of starch, accounts for hemicellulose, cellulose, and lignin, which are suitable for long-term acidogenic fermentation with a mixed microbial community (MMC). Overall, these results are in line with previous studies on melon, where another batch of the same variety was adopted (Costa et al., 2022). In another work performed by Greses and colleagues, where the melon was used to address short-chain fatty acids and hydrogen production, both melon dried matter and ashes calculated were comparable (91.8 g/L total solids and 9.3 %, respectively) while the VSS percentage was slightly larger (92.4 %) (Greses et al., 2021). Looking instead at the total nitrogen and protein measured, similar contents were accounted

Table 1
Physical and chemical characterization of melon waste used to feed AR. VSS: volatile suspended solids; COD: chemical oxygen demand; n.d.: not detected.

Particle size (μm)	<500 (90 %)	Cellulose (%) DM	17.2
Dried matter (DM) (%)	85.3	Hemicellulose (%) DM	3.3
Ashes (% of dried matter)	10.6	Lignin (%) DM	5.7
VSS (g/g)	0.75	Starch (%) DM	n.d.
COD (g(g)	0.97	Protein (%) DM	14.7
Total C (%)	41.5	Glucose (%) DM	13.7
Total N (%)	2.3	Fructose (%) DM	6.7
Total H (%)	6.8	Sucrose (%) DM	6.7

for (1.3 g/L cand 10.2 %, respectively).

3.2. Acidogenic continuous reactor

After the inoculum pre-treatment, the acidogenic reactor was run for 51 days under the optimized conditions previously described in the Materials & Method section. The resulting gas blend was composed of only H_2 and CO_2, since CH_4 production was completely inhibited thanks to the inoculum pre-treatment and BES supplementation. The reactor was considered stable when sugars were utterly consumed and biomass and effluents composition, in terms of bioconversion rate and gas production, were stationary. The bioconversion rate is obtained by dividing the COD of the VFAs and alcohols in the effluent with and the OL. Once stable conditions were reached, the OLR, in this study the pivotal variable, was increased to induce larger yields of H_2 and VFAs. Table 2 frames the overall performance of the AR, reporting data collected under stable conditions.

In the liquid effluent, glucose, fructose, and sucrose were detected only in negligible traces, whereas, on the other hand, total production of VFAs and alcohols increased progressively from 4.0 to 13.0 gCOD/L, thereby tripling, by increasing the OLR (Fig. 1A and Table 2). When VFAs and alcohol results are normalized for the OL, in other words by looking at the bioconversion rate, the raise is less accentuated but still widely significant: from an initial 40.3 %, the bioconversion rate ramped up gradually to 64.9 %. When compared to the outcomes from other related studies, these bioconversion rates underline the suitability of melon waste for dark fermentation applications (Küçükağa et al., 2022; Liu et al., 2018; Greses et al., 2021).

Similarly, total gas production increased broadly to reach 1.7 L/d, where H_2 and CO_2 fractions recorded 26.7 and 49.2 %, respectively (Table 2). To furtherly boost H_2 and CO_2 production the OLR again played a key role (Fig. 1B). The increase of OLR was followed, as demonstrated also by Paudel and colleagues who worked with food waste (Paudel et al., 2017), by larger % fractions of H_2 and CO_2 as well in the upper phase. Hence, besides working at larger scales, the OLR operating in the AR could be pushed to values higher than 20 gCOD/L/d, according to the limit of the feedstock itself: while dried melon has almost 1 of COD, a fresh melon is composed by 90 % of water which indeed allows theoretically to lift the OL to around 100 gCOD/L and potentially the OLR to even higher rates.

Regarding biomass fluctuations, lower SRT (and HRT) have been reported to entail larger H_2 yields, since H_2 consumer microbes growth would require longer SRT (Li and Yang, 2016). Similarly, when VFAs production is related to SRT, the optimization of this parameter follows a bell-shape behavior: below a specific threshold, very short SRT might cause cell washout, hence reducing VFAs production (Xiong et al., 2012). Indeed, results from Table 2 hint a still linear association between the drop in SRT and the increase in H_2 and CO_2 volumes and bioconversion rate. As further proof of the fact that the reactor was stable and biomass was not lost, the trends for OLR and VSS coupled and were not followed by a consistent increase in terms of F/M (Table 2 and Fig. 1C). In general, the increase of the OLR caused lower SRT yet larger biomass (VSS) and broader H_2 and CO_2 volumes and bioconversion rate as well (Fig. 1C).

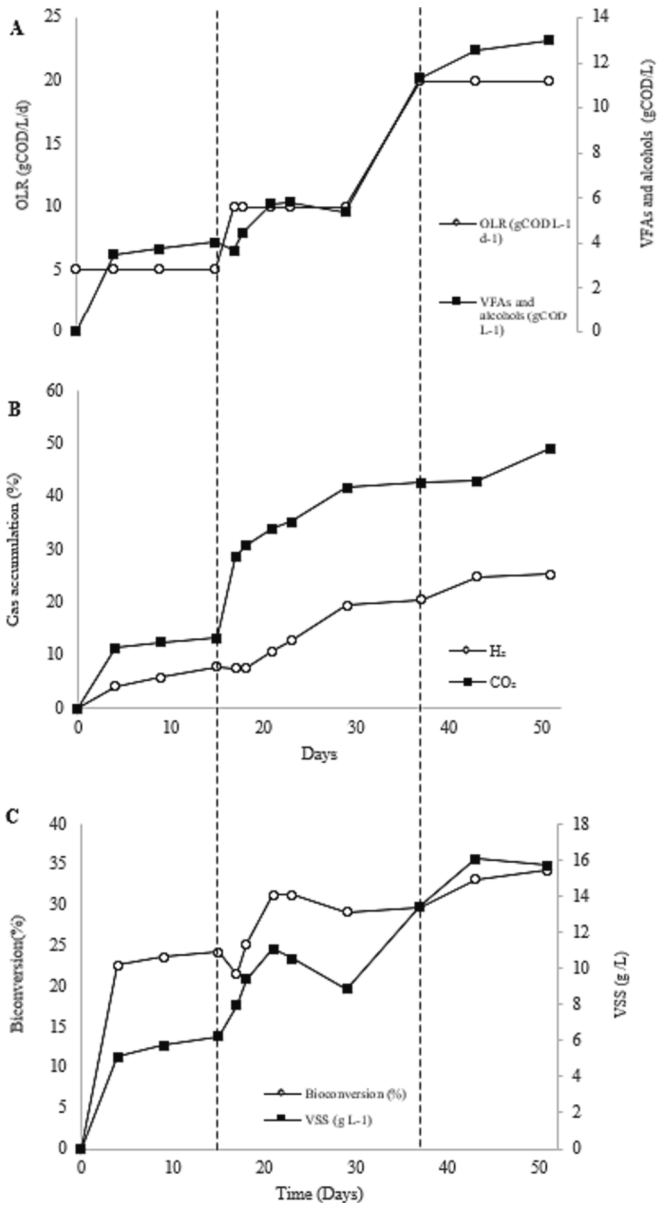

Fig. 1. A) Total VFAs and alcohols produced during 51 days of dark fermentation (gCOD/L) in black squares, OLR variations over time (gCOD/L/d) in white circles. B) Kinetics of H_2 (white circles) and CO_2 (black squares) percentages fractions in the headspace of the AR of melon waste. C) VSS (g/L) in black squares and Bioconversion rate (%) in white circles. Dotted vertical bars mark OLR changes. The data are the means of two replicates.

Hydrogen production via dark fermentation is a fast process. In a MMC, quick hydrogen-producing groups are dominant over slow ones and take advantage of the butyrate-acetate pathway (Lim and Nandong,

Table 2
Operational conditions of AR kept at pH 5.5 and 37 °C and results related to liquid effluent (sugars, VFAs and alcohols, and bioconversion rate) and gaseous stream at the end of each OLR tested condition, when the reactor was working under stable conditions. F/M, the food/microbe ratio, is obtained by dividing the OLR by the solids concentration that reflect the biomass concentration (gVSS/L, not reported). Sugars and gases data are the means of three replicates (±SD).

OL (gCOD/L)	HRT (d)	OLR (gCOD/L/d)	SRT (d)	F/M (gCOD/gVSS/d)	Sugars conversion (%)	VFAs and alcohols (gCOD/L)	Bioconversion (%)	H_2 and CO_2 (mL/d)	H_2 (% v/v)	CO_2 (% (v/v)
10.0	2.0	5.0	5.3	0.8	98.6±1.3	4.0	40.3	302.1±5.7	7.9±0.2	13.3±0.3
10.0	1.0	10.0	3.5	1.5	99.3±0.7	5.4	53.7	686.9±4.1	11.8 ±0.2	34.7±1.2
20.0	1.0	20.0	1.5	1.6	94.4±3.3	13.0	64.9	1860.3±12.3	26.7 ±0.4	49.2±1.4

2022). Indeed, looking at reactor kinetic within the first three hours after feeding (OLR 10 gCOD/L) (Fig. 2) immediate simple sugars depletion and simultaneous production of gas, VFAs and alcohols, can be appreciated by one hour. Afterwards, although glucose, fructose and sucrose are utterly consumed, H_2 and CO_2, VFAs and alcohols synthesis are curbed but not halted: whereas soluble sugars represent immediate substrates, it is likely that insoluble components such as cellulose, hemicellulose and lignin might instead be slowly processed by the MMC, hence explaining the uninterrupted productions of gas, VFAs and alcohols.

As already disclosed in Fig. 1A, VFAs and alcohols overall production increases according to OLR. Diving into details (Fig. 3), isopropanol recorded the highest concentrations among the detected soluble fermentation products, up to more than 4 gCOD/L. Similarly, Kim and colleagues noted the correlation between H_2 and isopropanol production using a MMC heated for 10 min at 90 °C, suggesting clostridial species as the main responsible for this specific alcohol production (Kim et al., 2008). As previously mentioned, the butyrate-acetate pathway is typical during the acidogenesis phase and hence the accumulation of these two acids is in line with expectations. On the other hand, propionic acid was first detected as OLR rose to 20 gCOD/L/d and finds a plausible explanation in the larger H_2 concentration since hydrogen itself is the precursor for propionic acid fermentation (Fuess et al., 2016). Similarly, to the trends of isopropanol and butyric acid, valeric acid and ethanol production increased following OLR higher values. Besides, as for propionic acid, isovaleric acid was detected in traces only when OLR was 20 gCOD/L/d. These results find support in another work, where these latter three metabolites trends proceeded in accordance with OLR (Hafez et al., 2010). Likewise for propionic acid, higher H_2 partial pressure might entail a metabolic veer towards reduced compounds such as butanol and ethanol (Castelló et al., 2020). While ethanol production was significant, butanol was measured only in traces when the reactor was operated at highest OLR tested.

3.3. PHAs production from acidogenic reactor gaseous and liquid streams

C. necator DSM 545 was then adopted in a two-step process to convert the two carbon-rich phases from the AR of waste melon, namely the gaseous stream or the liquid one into PHAs (Table 3 and Fig. 4). In the first step, *C. necator* DSM 545, once grown aerobically for 48 h using glucose (1 %) as a carbon source, produced up to 5.0 and 1.4 g/L of CDM and PHB, respectively. Bacterial cells were then transferred in the second step for the autotrophic (Fig. 4C) or heterotrophic (Fig. 4D) production of PHAs. Under both conditions, PHAs accumulation increased compared to the control experiment, where no carbon source was given during the second phase (Table 3). During autotrophic fermentation, *C. necator* DSM 545 accumulated up to 1.7 g/L of PHAs, which is 42 % larger than the benchmark condition (Table 3). As CO_2 represents the sole carbon source provided in the autotrophy experiments, the homopolymer P(3HB) represented 100 % of granules composition at the end of the fermentation. Specifically, when CO_2 and H_2 were sparged, 3HB biosynthesis enhanced in terms of intracellular PHAs content, from 31.7 to 37.8 % (Table 3). Additionally, as a consequence, cell-dried matter (CDM) values increased accordingly from 3.8 to 4.5 g/L. However, several parameters must be optimized to increase PHAs yields. Most importantly, it would be crucial to provide higher volumes of H_2 and CO_2, as already discussed. If one succeeds, a two-step continuum process for PHAs accumulation might be then conceived. Indeed, PHAs yields would ramp up as demonstrated when pure H_2 and CO_2 or syngas were provided uninterruptedly to *C. necator* (Garcia-Gonzalez et al., 2015; Garcia-Gonzalez and De Wever, 2017). Specifically, H_2 and CO_2 from the AR would be compressed and stored into a separate gasholder, as the balloon resembled in this work, to later be constantly sparged into the PHAs fermenter. At this point, it must be underlined the deepest advantage of this strategy and the rationale of the whole work: differently from the most common approaches adopting pure gases or syngas for autotrophic fermentations which imply either complex and expensive purification treatments or the presence of pollutants like CO, AR gaseous streams are tunable, cheap, and clean H_2 and CO_2 sources. These results are also interesting in the context of carbon capture, storage, and utilization (CCSU) which has a significant impact in reducing the emissions of CO_2. However, one of the critical points in the utilization of CO_2 is the availability of infrastructure for the distribution of this gas. In this sense, the direct conversion of CO_2 produced in one reactor, immediately used in a second one (as in this work, to produce PHAs) appears as a fast and efficient strategy (Kotagodahetti et al., 2021).

Differently, when the liquid fraction from the AR was used, 3HV monomer was detected too, since some precursors like propionic and valeric acid were part of the VFAs mixture (Table 3, Fig. 5). The presence of 3HV within the polymer chain renders the crystallinity and the melting point of the material lower, whereas flexibility and toughness

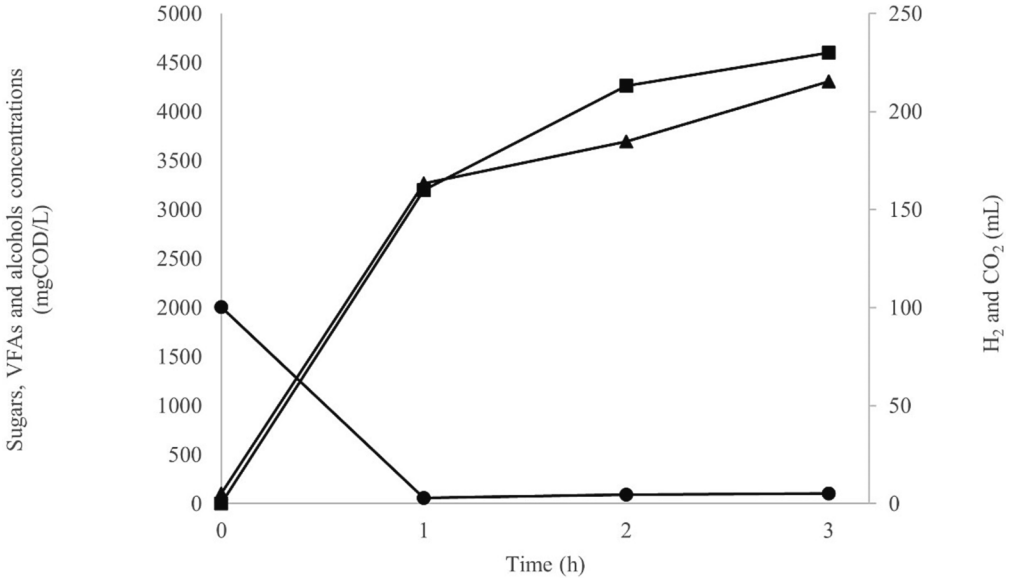

Fig. 2. AR short-time interval kinetic: soluble sugars consumption (circles) H_2 and CO_2 cumulative production (squares), and VFAs and alcohols production (triangles) within 3 h after feeding the reactor (OLR 10 gCOD/L/d). The data are the means of two replicates.

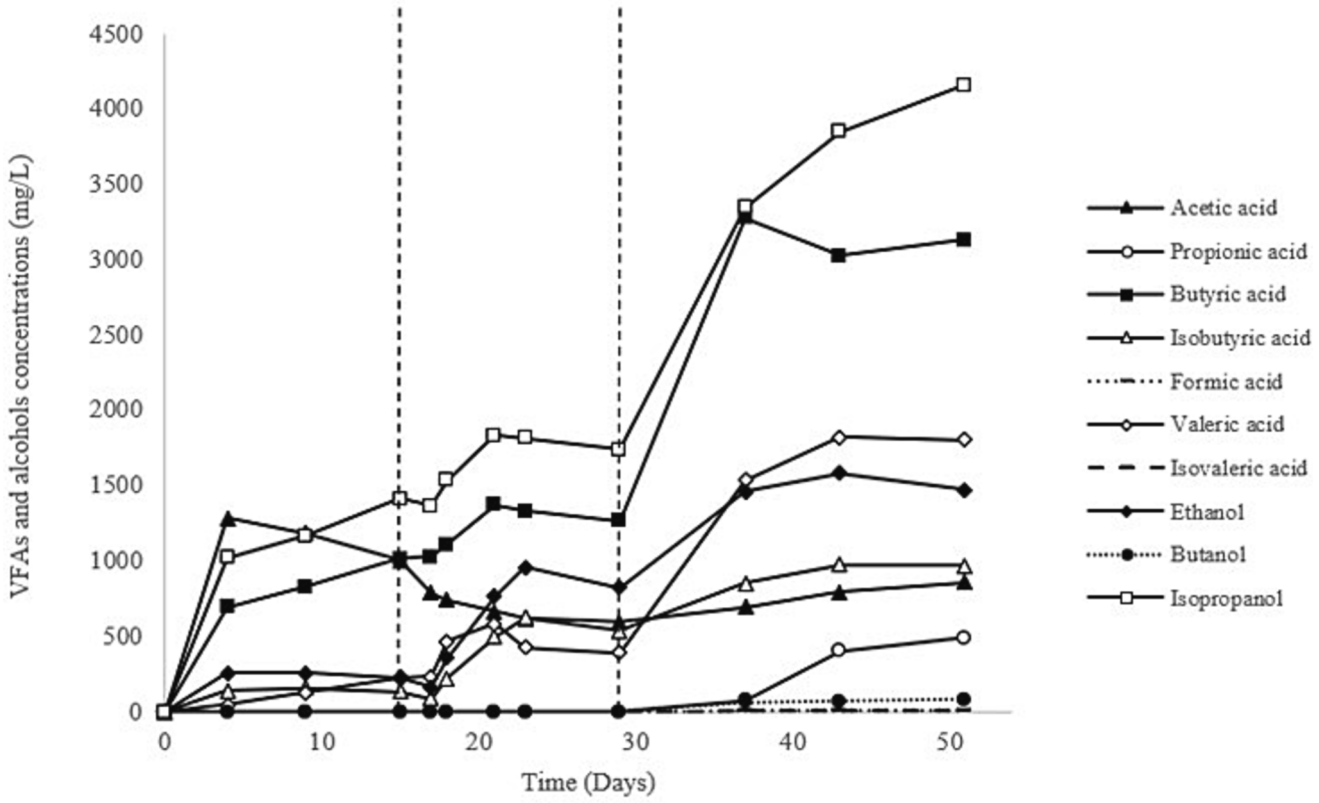

Fig. 3. VFAs and alcohols production profiles for 51 days fermentation in AR. Red bars represent OLR changes. The data are the means of two replicates.

Table 3
CDM and PHAs accumulation for *C. necator* DSM 545 after 96 h of fermentation under autotrophic or heterotrophic conditions. A benchmark was also conducted without providing the cells with any carbon source. (CTRL as a benchmark). PHAs values are expressed as total fraction of PHAs (% CDM) and both as concentrations and as fractions of 3HB and 3HV. The data are the means of three replicates (±SD).

	CDM (g/L)	PHAs (g/L)	PHAs (% CDM)	3HB (% PHAs)	3HV (% PHAs)
BENCHMARK	3.8 ±0.5	1.2±0.1	31.7±1.0	100	0.0
AUTOTROPHY	4.5 ±0.2	1.7±0.2	37.8±1.3	100	0.0
HETEROTROPHY	6.2 ±0.5	2.7±0.3	44.3±1.8	88.7	11.3

are enhanced (Min Song et al., 2022). PHAs accumulation reached 44.3 % of dried biomass, while, even more significantly, CDM peaked up to 6.2 g/L, suggesting PHAs production was combined with microbial growth due to the presence of nitrogen sources: overall 2.7 g/L of P (3HB-*co*-11.3 % 3HV) were produced. In the future, as proposed by Jawed and colleagues who adopted VFAs from an anaerobic digestor and artificial mixture of gases to produce PHAs (Jawed et al., 2022), a mixotrophic approach might be addressed: instead of using either the liquid or the gaseous stream from an AR both lines could be utilized in combination.

Glucose was chosen as a standard substrate for biomass growth during the first phase of fermentation. However, in another work, it was already reported the suitability of melon as an excellent feedstock for *C. necator* DSM 545 growth and accumulation of P(3HB-*co*-3HV) (Costa et al., 2022). It thus can be speculated that glucose-rich melon might display similar results concerning the initial growth phase. Diving now into the kinetics of the two-step PHAs process (Fig. 4), the patterns for the first 48 h are common for all the different tests, as experimental conditions were the same (Fig. 4A). On the other hand, during the accumulation phase, in the control case, the broth culture was deprived of both the carbon and nitrogen sources. As a result, CDM decreased from 5.0 to 3.8 g/L while PHAs concentration remained stable (Fig. 4B). However, when the gaseous mixture of H_2 and CO_2 was added in two intervals, PHAs production significantly rose (confirmed by OD_{600} measurements, data not shown) from 1.4 to 1.7 g/L (Fig. 4C). Samples collected from the headspace of the fermenter recorded no H_2 or CO_2, suggesting that both gases were either consumed or dissolved in the liquid phase (Fig. 4C). Moreover, 660 mL of H_2 and CO_2 (27 and 49 %, respectively) were supplemented twice, which if converted in grams accounts for 1.2 g of gas (mainly CO_2). As 0.4 g of PHAs were produced during the last 48 h, the yield in this process for PHAs accumulated to H_2 and CO_2 supplemented was thereby 0.34 g P(3HB)/gCO_2. Having in mind that when glucose is used as a substrate for PHAs production, the theoretical yield is 0.48 g/g, although practically this value ranges between 0.3 and 0.4, the results obtained in this work under autotrophic conditions gain significant relevance (Haas et al., 2017). Considering the volume of CO_2 produced at OLR 20 gCOD/L/d in the first reactor and the yield of P(3HB) from CO_2 just described, it can be concluded that the 2-step fermentation process recorded 30 mg P(3HB)/gCOD of melon. This result is comparable to others works where multi-step fermentation is adopted to produce PHAs. For instance, when combined treatment of organic fraction of municipal solid waste and sewage sludge were used, 65 g PHA/kg total volatile solids were obtained (Valentino et al., 2019). Differently, when liquid streams of the AR were used, under heterotrophic conditions, organic nitrogen concentration increased (Fig. 4D). Despite DSMZ-81 being prepared without NH_4Cl, organic nitrogen from acidogenesis liquid effluents exceeded what remained at the end of the growth phase. This, in combination with the VFAs and alcohols mixture, boosted both *C. necator* DSM 545 growth and P(3HB-*co*-3HV) accumulation. After 24 h of the second step, organic nitrogen dropped to zero and 74 % of VFAs and alcohols were already consumed, while acetic acid

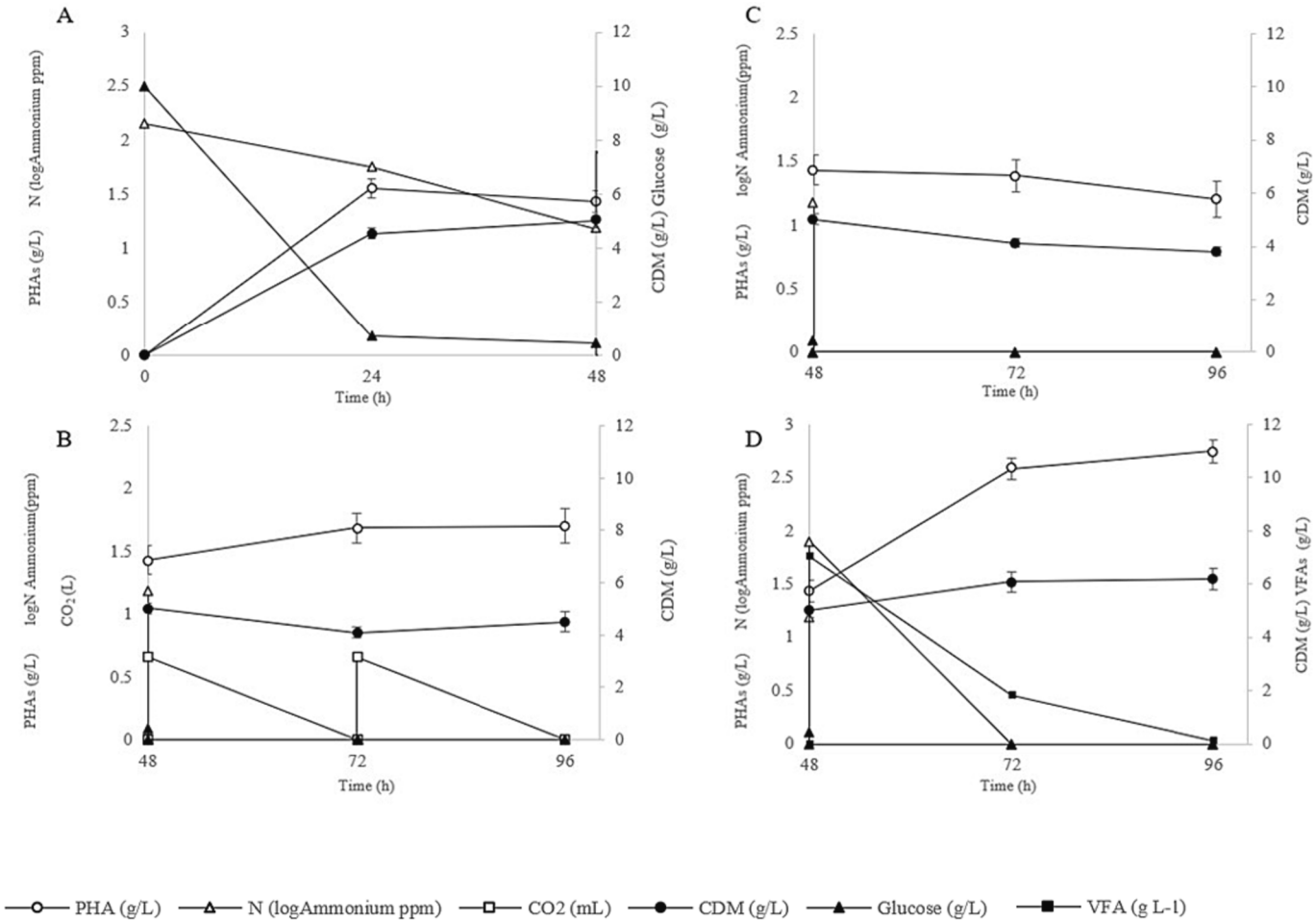

Fig. 4. *C. necator* DSM 545 fermentation kinetics. A) Average results of the common first 48 h for all the tested conditions; B) Second step – control condition; C) Second step – autotrophic condition; D) Second step – heterotrophic condition. Full triangles for glucose concentration (g/L); empty circles for PHAs (g/L); full circles for CDM (g/L); empty triangles for organic N (logAmmonium ppm); empty squares for CO_2 (L); full squares for VFAs and alcohols mix (g/L). The data are the means of three replicates (±SD).

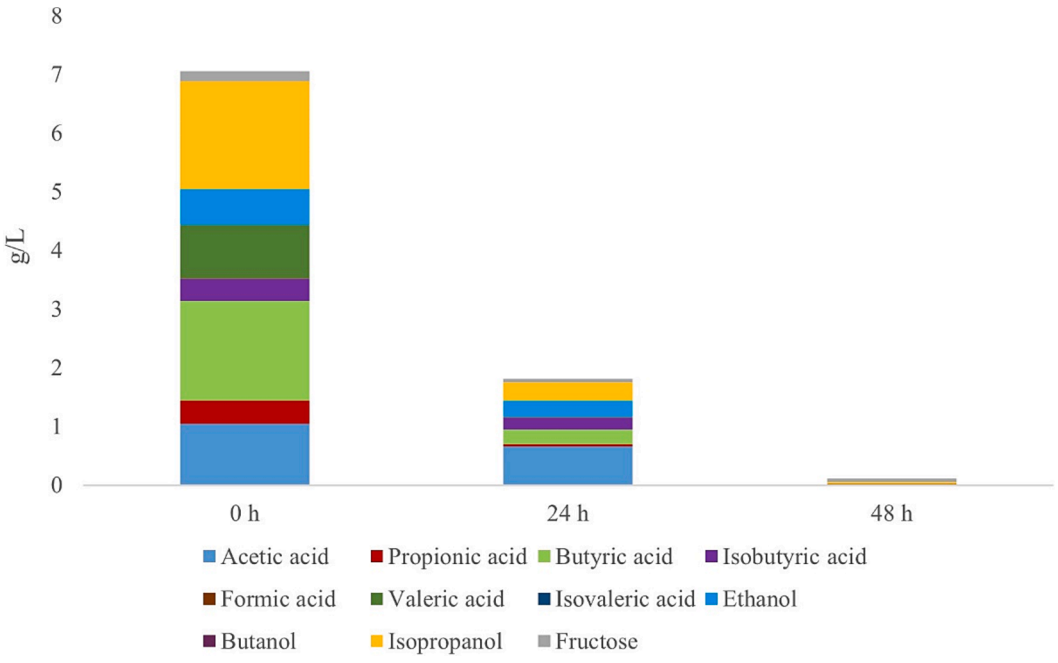

Fig. 5. VFAs and alcohols from AR consumption by *C. necator* DSM 545, after 24 and 48 h of fermentation during PHAs accumulation phase.

resulted as the slowest substrate to be assimilated by *C. necator* DSM 545 (Fig. 4D and Fig. 5). Eventually, within 48 h every carbon source was depleted and only traces were left. It can also be concluded that the other components not included in VFAs, alcohols, and organic nitrogen measurements didn't interfere with PHAs accumulation. Overall, as described in several papers and part already of industrial strategies, double-step production of PHAs from acidogenic fermentation-derived liquid effluents demonstrated here again great versatility (Brojanigo et al., 2022a; Koller and Mukherjee, 2022).

Altogether, the results represent first evidence and are proof-of-concept for the conversion of H_2 and CO_2 deriving from an acidogenic reactor fed with food waste. This work demonstrates the feasibility of the process that needs to be scaled up. By increasing the OLR in the AR, volumes of H_2 and CO_2 would enlarge accordingly and could be sparged continuously in the PHA reactor to support enhanced biopolymer accumulation. Additionally, the solubility of the gases could be enhanced by tailoring pivotal factors such as temperature and salinity. Further, melon waste could be adopted as sole feedstock to foster *C. necator* growth without the need for artificial media or carbon sources like DSMZ-81 and pure glucose. Finally, the liquid effluents from the AR might be used together with CO_2 and H_2, under a mixotrophic approach, to spike PHAs accumulation.

4. Conclusions

A two-step fermentation process was set up to convert acidogenesis-derived H_2 and CO_2, obtained by fruit wastes, into PHAs by *C. necator* DSM 545. The results represent the first evidence of autotrophic fermentation of H_2 and CO_2 originating from an AR into PHAs. Indeed, results, both in terms of yield (g P(3HB)/gCO_2) and increased concentration of PHAs under autotrophic conditions, were remarkable. Despite the mass transfer obstacles, this work is a proof of concept and demonstrates the feasibility of the approach, calling for future optimization, scale-up experiments, and techno-economical assessments.

Declaration of Competing Interest

The authors declare that they have no known competing financial interests or personal relationships that could have appeared to influence the work reported in this paper.

Data availability

Data will be made available on request.

Acknowledgements

This work was funded by Università degli Studi di Padova through BIRD210708/21 and DOR2352129/23 and Xunta de Galicia (Spain) through the Competitive Reference Research Groups grant (ED431C 2021/55 project).. The authors thank FRANCESCON OP SOC.AGR. SOC. CONS. a.r.l. for the donation of the melon waste. Additionally, the authors thank Professor Veiga and Professor Kennes's team for the technical support with the maintenance of bioreactors.

References

Abbondanzi, F., Biscaro, G., Carvalho, G., Favaro, L., Lemos, P., Paglione, M., Samorì, C., Torri, C., 2017. Fast method for the determination of short-chain-length polyhydroxyalkanoates (scl-PHAs) in bacterial samples by In Vial-Thermolysis (IVT). New Biotechnology 39 (2017), 29–35. https://doi.org/10.1016/j.nbt.2017.05.012.

Alibardi, L., Favaro, L., Lavagnolo, M.C., Basaglia, M., Casella, S., 2012. Effects of heat treatment on microbial communities of granular sludge for biological hydrogen production. Water Science and Technology 66, 1483–1490. https://doi.org/10.2166/wst.2012.336.

Basaglia, M., D'ambra, M., Piubello, G., Zanconato, V., Favaro, L., Casella, S., 2021. Agro-food residues and bioethanol potential: A study for a specific area. Processes 9, 1–15. https://doi.org/10.3390/pr9020344.

Bhatia, S.K., Otari, S.V., Jeon, J.M., Gurav, R., Choi, Y.K., Bhatia, R.K., Pugazhendhi, A., Kumar, V., Rajesh Banu, J., Yoon, J.J., Choi, K.Y., Yang, Y.H., 2021. Biowaste-to-bioplastic (polyhydroxyalkanoates): Conversion technologies, strategies, challenges, and perspective. Bioresource Technology 326, 124733. https://doi.org/10.1016/j.biortech.2021.124733.

Brojanigo, S., Parro, E., Cazzorla, T., Favaro, L., Basaglia, M., Casella, S., 2020. Conversion of starchy waste streams into polyhydroxyalkanoates using *Cupriavidus necator* DSM 545. Polymers 12, 1496.

Brojanigo, S., Alvarado-Morales, M., Basaglia, M., Casella, S., Favaro, L., Angelidaki, I., 2022a. Innovative co-production of polyhydroxyalkanoates and methane from broken rice. The Science of the Total Environment 825, 153931. https://doi.org/10.1016/j.scitotenv.2022.153931.

Brojanigo, S., Gronchi, N., Cazzorla, T., Wong, T.S., Basaglia, M., Favaro, L., Casella, S., 2022b. Engineering *Cupriavidus necator* DSM 545 for the one-step conversion of starchy waste into polyhydroxyalkanoates. Bioresource Technology 347, 126383. https://doi.org/10.1016/j.biortech.2021.126383.

Castelló, E., Nunes Ferraz-Junior, A.D., Andreani, C., Anzola-Rojas, M. del P., Borzacconi, L., Buitrón, G., Carrillo-Reyes, J., Gomes, S.D., Maintinguer, S.I., Moreno-Andrade, I., Palomo-Briones, R., Razo-Flores, E., Schiappacasse-Dasati, M., Tapia-Venegas, E., Valdez-Vázquez, I., Vesga-Baron, A., Zaiat, M., Etchebehere, C., 2020. Stability problems in the hydrogen production by dark fermentation: Possible causes and solutions. Renew. Sustain. Energy Rev. 119. https://doi.org/10.1016/j.rser.2019.109602.

Costa, P., Basaglia, M., Casella, S., Favaro, L., 2022. Polyhydroxyalkanoate Production from Fruit and Vegetable Waste Processing. Polymers (basel). 14 https://doi.org/10.3390/polym14245529.

Favaro, L., Alibardi, L., Lavagnolo, M.C., Casella, S., Basaglia, M., 2013. Effects of inoculum and indigenous microflora on hydrogen production from the organic fraction of municipal solid waste. International Journal of Hydrogen Energy 38, 11774–11779. https://doi.org/10.1016/j.ijhydene.2013.06.137.

Favaro, L., Basaglia, M., Casella, S., 2019. Improving polyhydroxyalkanoate production from inexpensive carbon sources by genetic approaches: a review. Biofuels. Bioprod. Biorefining 13, 208–227. https://doi.org/10.1002/bbb.1944.

Fuess, L.T., Mazine Kiyuna, L.S., Garcia, M.L., Zaiat, M., 2016. Operational strategies for long-term biohydrogen production from sugarcane stillage in a continuous acidogenic packed-bed reactor. International Journal of Hydrogen Energy 41, 8132–8145. https://doi.org/10.1016/j.ijhydene.2015.10.143.

Ganesh Saratale, R., Cho, S.K., Dattatraya Saratale, G., Kadam, A.A., Ghodake, G.S., Kumar, M., Naresh Bharagava, R., Kumar, G., Su Kim, D., Mulla, S.I., Seung Shin, H., 2021. A comprehensive overview and recent advances on polyhydroxyalkanoates (PHA) production using various organic waste streams. Bioresource Technology 325, 124685. https://doi.org/10.1016/j.biortech.2021.124685.

Garcia-Gonzalez, L., De Wever, H., 2017. Valorisation of CO2-rich off-gases to biopolymers through biotechnological process. FEMS Microbiology Letters 364, 1–8. https://doi.org/10.1093/femsle/fnx196.

Garcia-Gonzalez, L., Mozumder, M.S.I., Dubreuil, M., Volcke, E.I.P., De Wever, H., 2015. Sustainable autotrophic production of polyhydroxybutyrate (PHB) from CO2 using a two-stage cultivation system. Catalysis Today 257, 237–245. https://doi.org/10.1016/j.cattod.2014.05.025.

Geyer, R., Jambeck, J.R., Law, K.L., 2017. Production, use, and fate of all plastics ever made. Science Advances 3, 25–29. https://doi.org/10.1126/sciadv.1700782.

Greses, S., Tomás-Pejó, E., González-Fernández, C., 2021. Short-chain fatty acids and hydrogen production in one single anaerobic fermentation stage using carbohydrate-rich food waste. Journal of Cleaner Production 284. https://doi.org/10.1016/j.jclepro.2020.124727.

Haas, C., El-Najjar, T., Virgolini, N., Smerilli, M., Neureiter, M., 2017. High cell-density production of poly(3-hydroxybutyrate) in a membrane bioreactor. New Biotechnology 37, 117–122. https://doi.org/10.1016/j.nbt.2016.06.1461.

Hafez, H., Nakhla, G., El. Naggar, M.H., Elbeshbishy, E., Baghchehsaraee, B., 2010. Effect of organic loading on a novel hydrogen bioreactor. International Journal of Hydrogen Energy 35, 81–92. https://doi.org/10.1016/j.ijhydene.2009.10.051.

Jawed, K., Irorere, V.U., Bommareddy, R.R., Minton, N.P., Kovács, K., 2022. Establishing Mixotrophic Growth of *Cupriavidus necator* H16 on CO2 and Volatile Fatty Acids. Fermentation 8, 1–15. https://doi.org/10.3390/fermentation8030125.

Kim, S.H., Han, S.K., Shin, H.S., 2008. Optimization of continuous hydrogen fermentation of food waste as a function of solids retention time independent of hydraulic retention time. Process Biochemistry 43, 213–218. https://doi.org/10.1016/j.procbio.2007.11.007.

Koch, M., Spierling, S., Venkatachalam, V., Endres, H.J., Owsianiak, M., Vea, E.B., Daffert, C., Neureiter, M., Fritz, I., 2023. Comparative assessment of environmental impacts of 1st generation (corn feedstock) and 3rd generation (carbon dioxide feedstock) PHA production pathways using life cycle assessment. The Science of the Total Environment 863. https://doi.org/10.1016/j.scitotenv.2022.160991.

Koller, M., Mukherjee, A., 2022. A New Wave of Industrialization of PHA Biopolyesters. Bioengineering 9. https://doi.org/10.3390/bioengineering9020074.

Kotagodahetti, R., Hewage, K., Karunathilake, H., Sadiq, R., 2021. Evaluating carbon capturing strategies for emissions reduction in community energy systems: A life cycle thinking approach. Energy 232, 121012. https://doi.org/10.1016/j.energy.2021.121012.

Küçükağa, Y., Facchin, A., Kara, S., Naylr, T.Y., Scicchitano, D., Rampelli, S., Candela, M., Torri, C., 2022. Conversion of Pyrolysis Products into Volatile Fatty Acids with a Biochar-Packed Anaerobic Bioreactor. Industrial and Engineering Chemistry Research 61, 16624–16634. https://doi.org/10.1021/acs.iecr.2c02810.

Lambauer, V., Kratzer, R., 2022. Lab-Scale Cultivation of *Cupriavidus necator* on Explosive Gas Mixtures: Carbon Dioxide Fixation into Polyhydroxybutyrate. Bioengineering 9, 1–18. https://doi.org/10.3390/bioengineering9050204.

Lambauer, V., Permann, A., Petrášek, Z., Subotić, V., Hochenauer, C., Kratzer, R., Reichhartinger, M., 2023. Automatic Control of Chemolithotrophic Cultivation of *Cupriavidus necator*: Optimization of Oxygen Supply for Enhanced Bioplastic Production. Fermentation 9, 619. https://doi.org/10.3390/fermentation9070619.

Li, S., Yang, X., 2016. Biofuel production from food wastes. Handbook of Biofuels Production: Processes and Technologies: Second Edition. https://doi.org/10.1016/B978-0-08-100455-5.00020-5.

Lim, S.W., Nandong, J., 2022. Modeling of biohydrogen production using generalized multi-scale kinetic model: Impacts of fermentation conditions. International Journal of Hydrogen Energy 47, 17926–17945. https://doi.org/10.1016/j.ijhydene.2022.03.291.

Liu, C., Colón, B.C., Ziesack, M., Silver, P.A., Nocera, D.G., 2016. Water splitting–biosynthetic system with CO2 reduction efficiencies exceeding photosynthesis. Science 80-.). 352, 602–692. https://doi.org/10.1017/cbo9781139941785.014.

Liu, N., Jiang, J., Yan, F., Xu, Y., Yang, M., Gao, Y., Aihemaiti, A., Zou, Q., 2018. Optimization of simultaneous production of volatile fatty acids and bio-hydrogen from food waste using response surface methodology. RSC Advances 8, 10457–10464. https://doi.org/10.1039/c7ra13268a.

Liu, H., Saffaripour, M., Mellin, P., Grip, C.E., Yang, W., Blasiak, W., 2014. A thermodynamic study of hot syngas impurities in steel reheating furnaces - Corrosion and interaction with oxide scales. Energy 77, 352–361. https://doi.org/10.1016/j.energy.2014.08.092.

Min Song, H., Chan Joo, J., Hyun Lim, S., Jin Lim, H., Lee, S., Jae Park, S., 2022. Production of polyhydroxyalkanoates containing monomers conferring amorphous and elastomeric properties from renewable resources: Current status and future perspectives. Bioresource Technology 366, 128114. https://doi.org/10.1016/j.biortech.2022.128114.

Miyahara, Y., Yamamoto, M., Thorbecke, R., Mizuno, S., Tsuge, T., 2020. Autotrophic biosynthesis of polyhydroxyalkanoate by *Ralstonia eutropha* from non-combustible gas mixture with low hydrogen content. Biotechnology Letters 42, 1655–1662. https://doi.org/10.1007/s10529-020-02876-3.

Mukherjee, A., Koller, M., 2023. Microbial PolyHydroxyAlkanoate (PHA) Biopolymers—Intrinsically Natural. Bioengineering 10, 1–16. https://doi.org/10.3390/bioengineering10070855.

Müller, J., MacEachran, D., Burd, H., Sathitsuksanoh, N., Bi, C., Yeh, Y.C., Lee, T.S., Hillson, N.J., Chhabra, S.R., Singer, S.W., Beller, H.R., 2013. Engineering of *Ralstonia eutropha* H16 for autotrophic and heterotrophic production of methyl ketones. Applied and Environmental Microbiology 79, 4433–4439. https://doi.org/10.1128/AEM.00973-13.

Nangle, S.N., Ziesack, M., Buckley, S., Trivedi, D., Loh, D.M., Nocera, D.G., Silver, P.A., 2020. Valorization of CO2 through lithoautotrophic production of sustainable chemicals in *Cupriavidus necator*. Metabolic Engineering 62, 207–220. https://doi.org/10.1016/j.ymben.2020.09.002.

Obruca, S., Sedlacek, P., Koller, M., 2021. The underexplored role of diverse stress factors in microbial biopolymer synthesis. Bioresource Technology 326, 124767. https://doi.org/10.1016/j.biortech.2021.124767.

Panich, J., Fong, B., Singer, S.W., 2021. Metabolic Engineering of *Cupriavidus necator* H16 for Sustainable Biofuels from CO2. Trends in Biotechnology 39, 412–424. https://doi.org/10.1016/j.tibtech.2021.01.001.

Paudel, S., Kang, Y., Yoo, Y.S., Seo, G.T., 2017. Effect of volumetric organic loading rate (OLR) on H2 and CH4 production by two-stage anaerobic co-digestion of food waste and brown water. Waste Management. 61, 484–493.

Riegler, P., Chrusciel, T., Mayer, A., Doll, K., Weuster-Botz, D., 2019. Reversible retrofitting of a stirred-tank bioreactor for gas-lift operation to perform synthesis gas fermentation studies. Biochemical Engineering Journal 141, 89–101. https://doi.org/10.1016/j.bej.2018.09.021.

Rodríguez Gamero, J.E., Favaro, L., Pizzocchero, V., Lomolino, G., Basaglia, M., Casella, S., 2018. Nuclease expression in efficient polyhydroxyalkanoates-producing bacteria could yield cost reduction during downstream processing. Bioresource Technology 261 (2018), 176–181. https://doi.org/10.1016/j.biortech.2018.04.021.

Tagne, R.F.T., Costa, P., Casella, S., Favaro, L., 2023. Optimization of biohydrogen production by dark fermentation of African food-processing waste streams. International Journal of Hydrogen Energy. https://doi.org/10.1016/j.ijhydene.2023.07.348.

Tanaka, K., Ishizaki, A., Kanamaru, T., Kawano, T., 1995. Production of poly(D-3-hydroxybutyrate) from CO2, H2, and O2 by high cell density autotrophic cultivation of Alcaligenes eutrophus. Biotechnology and Bioengineering 45, 268–275.

Valentino, F., Moretto, G., Lorini, L., Bolzonella, D., Pavan, P., Majone, M., 2019. Pilot-Scale Polyhydroxyalkanoate Production from Combined Treatment of Organic Fraction of Municipal Solid Waste and Sewage Sludge. Industrial & Engineering Chemistry Research. 58, 12149–12158.

Waghmode, T.R., Haque, M.M., Kim, S.Y., Kim, P.J., 2015. Effective suppression of methane emission by 2-bromoethanesulfonate during rice cultivation. PLoS One1 10, 1–13. https://doi.org/10.1371/journal.pone.0142569.

Xiong, H., Chen, J., Wang, H., Shi, H., 2012. Influences of volatile solid concentration, temperature and solid retention time for the hydrolysis of waste activated sludge to recover volatile fatty acids. Bioresource Technology 119, 285–292. https://doi.org/10.1016/j.biortech.2012.05.126.

Yadav, B., Pandey, A., Kumar, L.R., Tyagi, R.D., 2020. Bioconversion of waste (water)/residues to bioplastics- A circular bioeconomy approach. Bioresource Technology 298, 122584. https://doi.org/10.1016/j.biortech.2019.122584.

Yoon, J., Oh, M.K., 2022. Strategies for Biosynthesis of C1 Gas-derived Polyhydroxyalkanoates: A review. Bioresource Technology 344, 126307. https://doi.org/10.1016/j.biortech.2021.126307.

Yukesh Kannah, R., Dinesh Kumar, M., Kavitha, S., Rajesh Banu, J., Kumar Tyagi, V., Rajaguru, P., Kumar, G., 2022. Production and recovery of polyhydroxyalkanoates (PHA) from waste streams – A review. Bioresource Technology 366, 128203. https://doi.org/10.1016/j.biortech.2022.128203.